

Resonant second-harmonic generation on Cu(111) by a surface-state to image-potential-state transition

G. Lüpke*

Institut für Laser- und Plasmaphysik, Universität-GHS-Essen, 45117 Essen, Germany

D. J. Bottomley and H. M. van Driel

Department of Physics and Ontario Laser and Lightwave Research Centre, University of Toronto, Toronto, Ontario, Canada M5S 1A7

(Received 10 November 1993)

Dispersion measurements of second-harmonic generation from a clean Cu(111) surface show a resonance feature at the second-harmonic (SH) photon energy of 4.1 eV, consistent with an image-potential-state to surface-state transition in agreement with polarization selection rules. The sensitivity of the SH efficiency to surface defects on Cu(111), observed by Bloch *et al.* [Phys. Rev. B **45**, 12 011 (1992)], is explained in terms of an inherent energy broadening of the surface-state wave function.

Second-harmonic (SH) generation is a powerful probe of the electronic and structural properties of interfaces between centrosymmetric media.¹⁻³ For the vacuum-metal interface, significant progress has been made in our understanding of the response of simple “jelliumlike” metals such as aluminum, for which theoretical^{4,5} and experimental work^{6,7} has provided much insight into the spatial distribution of electrons at the interface and their nonlinear optical response. However, it is well known that most metal surfaces possess various types of intrinsic or defect surface states as well as image-potential bound states. These interface states should enhance the second-order nonlinear optical susceptibility $\chi^{(2)}$ when the fundamental photon energy $\hbar\omega$, or second harmonic photon energy $2\hbar\omega$, is resonant with an electric dipole-allowed transition.⁸ There have been several reports of surface-state enhancement of $\chi^{(2)}$ not only on metals, but also at semiconductor interfaces.^{12,13} The identification of these states on certain metal surfaces through nonlinear optical techniques was ambiguous, however, either because spectroscopic investigations were not conducted or the interfacial electronic properties were not known. For the Ag(111) surface, a resonance in the SH response has been detected near $2\hbar\omega=3.8$ eV.^{9,10} However, it has been shown that this is dominated by, if not entirely due to, enhancement of SH fields by a resonance in the linear susceptibility $\chi^{(1)}$ rather than effects intrinsic to $\chi^{(2)}$.¹¹ Perhaps the only example to date of an enhancement of $\chi^{(2)}$ states on a metal surface is that observed on Ag(110) where a maximum in the SH intensity at $\hbar\omega=1.73$ eV was assigned to a transition between intrinsic states in a region where the linear optical properties are not dispersive.¹¹

Here we present observations of a resonant enhancement of $\chi^{(2)}$ from a metal by an image-potential-state to surface-state transition. This conclusion is reached from a systematic experimental investigation of SH generation from a clean Cu(111) surface as a function of photon energy and crystal azimuthal orientation. Cu(111) is a good candidate for investigating possible surface-state-induced

resonances in $\chi^{(2)}$ because the occupied and unoccupied surface-state energies have been measured and calculated.¹⁴⁻¹⁶ Furthermore, in the spectral region covered here, namely, $1.6 < \hbar\omega < 2.1$ eV ($3.2 < 2\hbar\omega < 4.2$ eV), there are no resonances in $\chi^{(1)}$.¹⁷ We also suggest that earlier observations of the sensitivity of the SH intensity yielded by Cu(111) at $2\hbar\omega=4.1$ eV to lattice temperature and Ar-ion surface bombardment¹⁸ can be explained by a linewidth broadening associated with electrons in surface states scattering into bulk states, consistent with angle-resolved photoemission measurements.

A 1-cm-diam, 2-mm-thick Cu(111) sample was mounted in an ultrahigh vacuum chamber (5×10^{-10} Torr base pressure) on a manipulator, which was used to vary the azimuthal orientation of the sample. The surface was prepared using sputtering and annealing techniques; surface crystalline order and cleanliness were monitored using low-energy electron-diffraction and Auger-electron spectroscopy. For the SH dispersion measurements, we used a synchronously pumped mode-locked dye laser, which produced a train of 3-ps pulses at 76 MHz with an average power of 200–500 mW. With three different dyes, the fundamental wavelength range 775–590 nm ($1.6 < \hbar\omega < 2.1$ eV) could be covered. A *p*-polarized beam was focused to a 40- μ m-diam spot on the sample at an angle of incidence θ of 67°, and *p*-polarized SH light was detected in reflection using a photomultiplier tube and conventional photon-counting techniques. Approximately 5% of the laser beam was split off and used to generate SH in a quartz crystal as a reference. Details of the experimental apparatus and measurement techniques are given in Ref. 6.

Figure 1 shows the reflected SH efficiency R of the sample as a function of wavelength obtained for two azimuthal orientations ψ of the sample. Here ψ is the angle between the plane of incidence and the $[\bar{1}12]$ axis. The efficiency depends on ψ as given by

$$R \propto |\chi_{\text{eff}}^{(2)}|^2 = |A + B \cos(3\psi)|^2 \quad (1)$$

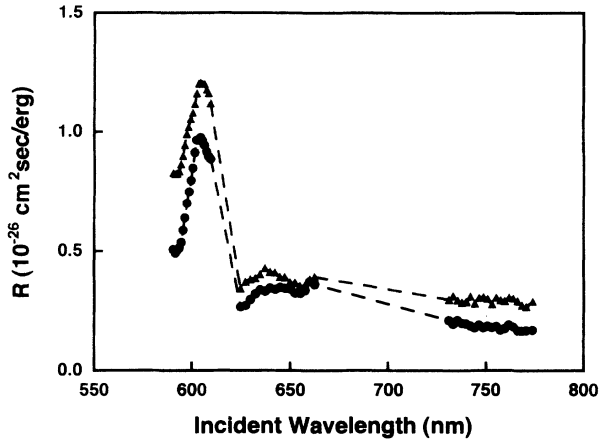


FIG. 1. The p -polarized SH efficiency R of the clean Cu(111) surface as a function of the wavelength of p -polarized fundamental light incident at 67° . The sample temperature was 320 K. Data set (a) (\blacktriangle) was obtained for the maximum intensity at azimuthal position $\psi=0^\circ$; data set (b) (\bullet) was taken at $\psi=30^\circ$. The dashed curves are guides to the eye.

for a surface with C_{3v} symmetry.¹⁹ The $\chi_{\text{eff}}^{(2)}$ is the effective second-order nonlinear susceptibility, and A and B are linear combinations of $\chi_{ijk}^{(2)}$ tensor elements multiplied by angle-of-incidence-dependent Fresnel factors.¹⁹ Figure 1 shows R for $\psi=0^\circ$ where one expects $R \propto |A+B|^2$, and for $\psi=30^\circ$ where $R \propto |A|^2$. Thus, we can directly derive the SH photon energy dependence of $|A|$ and this is shown in Fig. 2. From the SH rotational anisotropy as shown by Bloch *et al.*,¹⁸ the phase difference between A and B is small ($<20^\circ$), resulting in the observed threefold modulation of the SH intensity as a function of ψ . By neglecting the phase difference between A and B and removing the contribution of $|A|$ from data set (a) in Fig. 1, we obtain the SH photon energy dependence of $|B|$ which is shown in Fig. 2.

It is clear from Fig. 2 that the maximum in the SH response near 600 nm in Fig. 1 is almost entirely due to a resonance in the isotropic coefficient A ; the anisotropic coefficient B does not offer any strong evidence for such a feature in the energy range considered since it varies only slowly with SH photon energy. The coefficient A contains contributions from the surface susceptibility tensor elements $\chi_{zzz}^{(2)}$, $\chi_{xxx}^{(2)}$, and $\chi_{xzz}^{(2)}$, the isotropic bulk quadrupolar response, and the linear optical parameters of the material; surface contributions to B arise from $\chi_{xxx}^{(2)}$

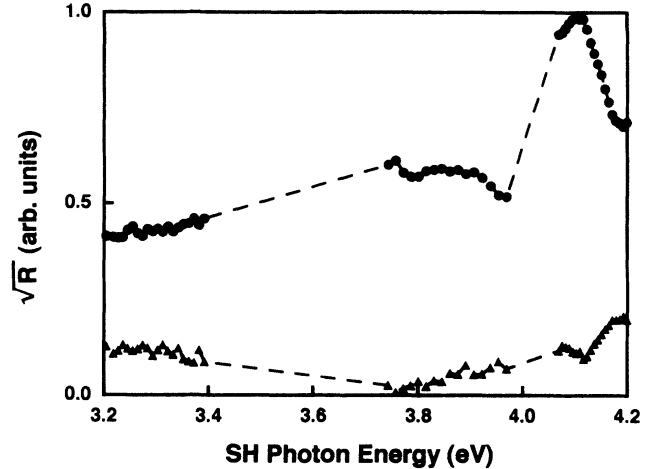


FIG. 2. $|A|$ (\bullet) and $|B|$ (\blacktriangle) as a function of SH photon energy. The dashed curves are guides to the eye.

terms.¹⁹ Here, the x axis lies in the crystal-surface plane and in the plane of incidence for $\psi=0^\circ$, and the z axis is normal to the crystal surface. Linear optical effects can be excluded as a source of the observed SH resonance as they contribute similarly to both A and B .¹⁹ Furthermore, Bloch *et al.*²⁰ found that during exposure of the Cu(111) surface to oxygen, the SH intensity drops by a factor of 10 at wavelengths in the vicinity of the resonance. Therefore, the isotropic bulk electric quadrupole contribution is relatively small at $2\hbar\omega=4.1$ eV. Finally, the strong increase of the SH efficiency with increasing angle of incidence θ strongly suggests that the surface susceptibilities $\chi_{zzz}^{(2)}$ and $\chi_{xzz}^{(2)}$, which dominate the SH response for small θ , can be neglected here.¹⁹ Thus, the strongest candidate for the resonance at $2\hbar\omega=4.1$ eV is the $\chi_{zzz}^{(2)}$ tensor element.

In general the surface $\chi^{(2)}$ arises from two sources. The first is related to a "jellium" electron contribution and its strength and dispersion characteristics have been widely discussed in the literature.⁴⁻⁷ The second is related to electrons in true surface states, whose characteristics are particular to the metal and symmetry of the surface. A comparison of the experimental data with the broad dispersion characteristics of the SH response predicted by the jellium model⁵ shows that the experimental resonant feature is too narrow in energy to arise from this source. We, therefore, attribute the resonantly enhanced $\chi^{(2)}$ to transitions of electrons between surface states. The general form of $\chi^{(2)}$ can be written as²¹

$$\chi_{ijk}^{(2)}(-2\omega; \omega, \omega) = N \frac{e^3}{\epsilon_0 \hbar^2} S \sum_{l,m,n} \rho_{ll} \frac{\langle l | r_i | n \rangle \langle n | r_j | m \rangle \langle m | r_k | l \rangle}{(2\hbar\omega - E_{nl} - i\hbar\gamma_{nl})(\hbar\omega - E_{ml} - i\hbar\gamma_{ml})}, \quad (2)$$

where r_i is the Cartesian coordinate operator, N is the electron density, ρ_{ll} is the equilibrium density matrix, E_{nl} is the energy separation between electronic states $|l\rangle$ and $|n\rangle$, and γ_{nl} is half of the linewidth of the $|l\rangle \rightarrow |n\rangle$ transition: S indicates that the following expression should be summed over permutations of beam

polarization-frequency pairs.

We now consider the possible transitions which can contribute to the observed SH generation behavior. Figure 3 shows¹⁵ experimental and theoretical dispersion relations $E(k_{\parallel})$ in the surface Brillouin zone for the projected bulk continuum bands, the $n=1$ member of a

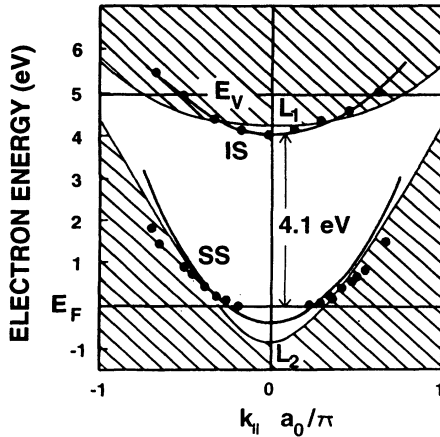


FIG. 3. Surface-projected band structure for Cu(111) adapted from Ref. 15. The cross-hatched area is the projection of the bulk band structure. The Fermi and vacuum energy levels are indicated by E_F and E_V ; IS indicates the $n=1$ image state while SS indicates the Gartland-Slagsvold surface state (see text). ● corresponds to data taken from Ref. 15.

Rydberg series of image-potential surface states (IS), and for the surface state (SS) originally observed by Gartland and Slagsvold.¹⁶ The s -band-edge continuum states (L_1) are approximately 4.3 eV above the Fermi level and are too high in energy to be involved in a resonant excitation emission with the photon energies used in these studies. However, near the $\bar{\Gamma}$ point IS, which is pinned to the vacuum level, is located near the top of the band gap just below L_1 . By taking the average values for the work function of Cu(111) and the binding energy of IS (from Table I of Ref. 22) to be 4.92 and 0.82 eV, respectively, we estimate an energy separation between IS and E_F of 4.1 eV. Note that in Ref. 22, the estimated error of the 4.1-eV energy separation between IS and E_F is ± 0.15 eV. The IS are ideally suited for second-order nonlinear optical processes. A significant population can be produced because of their long lifetime which is a consequence of their location outside the solid.

We now focus on the polarization selection rules for possible transitions involving IS and various states located at an energy of 4.1 eV below it. Consider first the surface state, which exists along the $\bar{\Gamma}$ - L line in the surface Brillouin zone. Its binding energy at $\bar{\Gamma}$ is -0.4 eV relative to the Fermi energy E_F , and it disperses parabolically upward (effective mass $0.42m_0$) and approaches the bulk continuum near E_F as shown in Fig. 3.^{14,16} Gartland and Slagsvold¹⁶ demonstrated in their photoemission spectra that electrons in SS are excited only when the linearly polarized light has an electric field with a component normal to the surface.²³ Giesen *et al.* identified the transition between SS and IS as the dominant process in two-photon photoemission using p -polarized light.²⁴ No photoemission was seen with s polarization in agreement with selection rules for transitions involving these states.²⁴ The same polarization selection rules also exist for inverse photoemission²² (in which photons are emitted, and not absorbed as a photoemission) and where a

resonance is observed at 4.1 eV, corresponding to a final state near the Fermi level. It is possible that, because of the large effective mass [$> m_0$ (Ref. 22)] of the $n=1$ image potential state, and the uncertainty in its binding energy, transitions can occur between IS and SS at 4.1 eV and satisfy conservation of k_{\parallel} . Finally, it is also possible that transitions can occur between IS and the bulk bands with sp character that are projected onto the surface.²⁵ These also satisfy the selection rules.

Jiang, Pajer, and Burstein⁸ have suggested that an additional three-step process may contribute to $\chi^{(2)}$. An electron in the SS exhibiting a mostly p_z character makes an E_z -induced transition to a p -type continuum state L_2 , where E_z is the z component of the electric field. In the second step the electron is excited to IS by E_z , creating an electron and a hole in SS. In the third step the excited electron-hole ($e-h$) pair recombines, emitting a photon with an E_z component. A second three-step process is also possible. This involves an intraband transition of an electron in L_2 , induced by E_z , creating an $e-h$ pair in the first step; a $L_2 \rightarrow$ IS interband transition of the excited electron induced by E_z , and the scattering of an electron from SS into L_2 completes the second step. Finally, the recombination of the excited electron in IS with the excited hole in SS leads to a z -polarized SH photon.

The above processes all contribute to $\chi_{zzz}^{(2)}$ and their frequency-dependent contributions will exhibit an onset when the frequency of the SH photon corresponds to the energy separation between IS and E_F . These are the most likely contributors to the resonance in A at $2\hbar\omega=4.1$ eV. Furthermore, these processes cannot contribute to the anisotropic coefficient B which arises from $\chi_{xxx}^{(2)}$ and the bulk quadrupole anisotropic contribution.¹⁹ We can gain further insight into the processes contributing to the observed SH resonance by comparing our full width at half maximum (FWHM) ~ 200 meV of $\chi_{zzz}^{(2)}$ at $2\hbar\omega=4.1$ eV with the peak widths in photoemission spectra. The resonance at 4.46 eV in the Cu(111) two-photon photoelectron spectrum taken at $k_{\parallel}=0$, which is associated with the same $n=1$ Rydberg state above E_F , exhibits a FWHM of ~ 150 meV (Fig. 2 of Ref. 24). High-resolution angle-resolved photoemission measurements of the SS on Cu(111) demonstrates that its peak width increases from 70 meV at $k_{\parallel}=0$ to ~ 200 meV near E_F , a result contrary to the usual expectations based on final-state lifetimes.¹⁴ Kevan explained the broadening mechanism by considering SS as a defect-induced state, which interacts more strongly with the bulk states as its energy approaches that of the bulk continuum near E_F . This mechanism requires that the transition from surface state to surface resonance is gradual and dependent upon the degree to which the surface-state wave function penetrates the bulk, a fact demonstrated powerfully by Hulbert *et al.* using k -resolved inverse photoemission spectroscopy (cf. Ref. 15 with Fig. 3). The SS are energy broadened because of the probability of electrons localized in SS being scattered into bulk states. These scattering events cannot conserve k_{\parallel} and hence must be inelastic or defect assisted. This explanation is consistent with the SH efficiency of Cu(111) at 4.1 eV being sensitive to the

density of surface defects. From Eq. (2), a defect-induced broadening of the half-linewidths γ_{nl} or γ_{ml} will lead to a decrease in the SH efficiency, which in fact has been observed by Bloch *et al.* after sputtering or heating of the Cu(111) surface.¹⁸

We have shown that the observed SH resonance at 4.1 eV is due to a coupling between the SH photon and an electronic transition between the lowest-energy image-potential state and surface states near the Fermi level. Further SH dispersion measurements of higher order ($n > 1$) IS combined with femtosecond pump-probe tech-

niques should provide information about the dynamics of these states and their coupling to the crystal lattice. The studies are of particular interest since a confined two-dimensional electron gas can exhibit novel transport properties.

We gratefully acknowledge financial support from the Natural Sciences and Engineering Research Council of Canada and the Ontario (Canada) High Technology fund. We thank Dr. S. Janz for helpful discussions on absolute SH generation measurements.

*Present address: Institut für Halbleitertechnik II, RWTH-Aachen, Sommerfeldstr. 24, D-52074 Aachen, Germany.

¹Y. R. Shen, *Nature* (London) **337**, 519 (1989).

²G. L. Richmond, J. M. Robinson, and V. L. Shannon, *Prog. Surf. Sci.* **28**, 1 (1987).

³G. Lüpke, D. J. Bottomley, and H. M. van Driel, *Phys. Rev. B* **47**, 10 389 (1993).

⁴J. Rudnick and E. A. Stern, *Phys. Rev. B* **4**, 4274 (1971).

⁵A. Liebsch and W. L. Schaich, *Phys. Rev. B* **40**, 5401 (1989).

⁶S. Janz, W. Pedersen, and H. M. van Driel, *Phys. Rev. B* **44**, 3943 (1991).

⁷R. Murphy, M. Yeganeh, K. J. Song, and E. W. Plummer, *Phys. Rev. Lett.* **63**, 318 (1989).

⁸M. Y. Jiang, G. Pajer, and E. Burstein, *Surf. Sci.* **242**, 306 (1991).

⁹K. Giesen, F. Hage, H. J. Reiss, W. Steinmann, R. Haight, R. Beigang, R. Dreyfus, Ph. Avouris, and F. J. Himpsel, *Phys. Scr.* **35**, 578 (1987).

¹⁰R. A. Bradley, R. Georgiadis, S. D. Kevan, and G. L. Richmond, *J. Vac. Sci. Technol. A* **10**, 2996 (1992).

¹¹L. E. Urbach, K. L. Percival, J. M. Hicks, E. W. Plummer, and H. L. Dai, *Phys. Rev. B* **45**, 3769 (1992).

¹²T. F. Heinz, F. J. Himpsel, E. Palange, and E. Burstein, *Phys. Rev. Lett.* **63**, 644 (1989).

¹³M. S. Yeganeh, J. Qi, A. G. Yodh, and M. C. Tamargo, *Phys. Rev. Lett.* **69**, 3579 (1992).

¹⁴S. D. Kevan, *Phys. Rev. Lett.* **50**, 526 (1983).

¹⁵S. L. Hulbert, P. D. Johnson, N. G. Stoffel, W. A. Royer, and

N. V. Smith, *Phys. Rev. B* **31**, 6815 (1985).

¹⁶P. O. Gartland and B. J. Slagsvold, *Phys. Rev. B* **12**, 4047 (1975).

¹⁷*Handbook of Optical Constants of Solids*, edited by E. D. Palik (Academic, Orlando, 1985).

¹⁸J. Bloch, G. Lüpke, S. Janz, and H. M. van Driel, *Phys. Rev. B* **45**, 12 011 (1992).

¹⁹J. E. Sipe, D. J. Moss, and H. M. van Driel, *Phys. Rev. B* **35**, 1129 (1987).

²⁰J. Bloch, D. J. Bottomley, S. Janz, and H. M. van Driel, *Surf. Sci.* **257**, 328 (1991).

²¹See, for example, P. N. Butcher and D. Cotter, *Elements of Nonlinear Optics* (Cambridge University Press, Cambridge, 1990).

²²D. Straub and F. J. Himpsel, *Phys. Rev. B* **33**, 2256 (1986).

²³In the terminology used by Giesen *et al.* (Ref. 24) the occupied Λ_1 surface state which is located 0.41 eV below the Fermi level corresponds to the Gartland-Slagsvold surface state, and is often referred to as the $n=0$ member of the series of image-potential surface states [M. Weinert, S. L. Hulbert, and P. D. Johnson, *Phys. Rev. Lett.* **55**, 2055 (1985)]. The first unoccupied Λ_1 surface state corresponds to the first image-potential surface state.

²⁴K. Giesen, F. Hage, F. J. Himpsel, H. J. Riess, and W. Steinmann, *Phys. Rev. B* **33**, 5241 (1986).

²⁵S. D. Kevan and R. H. Gaylord, *Phys. Rev. Lett.* **57**, 2975 (1986); *Phys. Rev. B* **36**, 5809 (1987).